Ring laser detection of rotations from teleseismic waves

A. Pancha, T. H. Webb

Institute of Geological and Nuclear Sciences, Lower Hutt, New Zealand

G. E. Stedman, D. P. McLeod

Department of Physics and Astronomy, University of Canterbury, Christchurch, New Zealand

K. U. Schreiber

Fundamentalstation Wettzell, Kötzting, Germany

Abstract. Horizontal and vertical rotational components of teleseismic surface and body waves are detected by large ring laser gyroscopes. This is illustrated with records from magnitudes 7.0 and 7.3 events at distances of 31 deg. and 42.6 deg. respectively. Phase comparisons with synchronous linear seismometer records confirm the gyroscopic coupling.

Introduction

Large ring laser gyroscopes detect the local rotational effects of seismic waves. This was shown for a 1995 regional earthquake using a large ring laser system C-I in a cavern 30 m underground at Cashmere, Christchurch [*Stedman et al.*, 1995]. In a later work [*McLeod et al.*, 1998], a fuller analysis was given of the C-I record of a 1996 regional earthquake. Possible coupling mechanisms were evaluated, rotational coupling being estimated to dominate strain and tilt strongly. The geophysical interest of such measurements includes establishing the frequency dependence of seismic rotation in different situations, analysing mode conversion, and determining the spatial variation of slip velocity over the fault planes of local events [*Takeo and Ito*, 1997]. In engineering, the relationship between ground rotation and induced building rotation has interest for establishing the frequency dependence of building response to rotation in the 0.2–30 Hz band.

C-I has a simple construction with mirrors mounted on a low-expansion ceramic (Zerodur) table, an area of 0.755 m^2, a quality factor Q $\sim$7.5 $\times 10^{10}$, and a sensitivity for rotation detection $S \sim 6$ nrad/$\sqrt{}$Hz [*Stedman*, 1997]. We report here the successful extension of this to the detection of teleseismic waves (of period $\sim$ 18-22 seconds) in two more advanced square HeNe ring lasers C-II and G0 now at Cashmere. As we show, the noise floor is significantly below that for reported rotational accelerometers [*Luiten et al.*, 1997]. The increase in sensitivity over our earlier work is associated with better engineering (for C-II) or with greater size (for G0); C-II has a monolithic construction in a solid piece of Zerodur (˜0.65 tonne), a beam area of 1 m^2, and a quality factor 6×10^{12} [*Stedman*, 1997], and G0 has a simple construction, area 12.25 m^2 [*Rowe et al.*, 1999]. C-II, locally horizontal, measures the rotation rate about the local vertical, and so naturally detects SH or Love wave rotation, while G0, mounted vertically on a cavern wall, measures the rotation rate about a horizontal axis 9° west of north, and so naturally detects SV or Rayleigh wave rotation.

Other major improvements were important in securing the present results. Linear seismometer output is recorded synchronously with ring laser output, eliminating uncertainties of relative timing, and allowing a novel phase comparison. C-II and G0 were upgraded during December 1998 to new mirrors and a more symmetric cavity geometry. A prediction [*Schreiber et al.*, 1999] that this would reduce backscatter-induced frequency drift was dramatically fulfilled, frequency stability being improved by a factor of order 100, with Allan deviations relative to the Sagnac frequency from Earth rotation (79 Hz in C-II, 288 Hz in G0) as low as 1 $\times 10^{-6}$ for C-II at 1000 sec sampling times and 5×10^{-6} for G0 at 300 sec sampling times [*Schreiber et al.*, 1999b]. Second-order autoregression (AR[2]) estimation of the Sagnac frequency has proved to be highly suited to seismic analysis (McLeod *et al.* in preparation), more rapid and efficient than our previous (Fourier or analytic phase) methods, when as here the data is quantum noise-limited; it gives accuracies of a few millihertz in the base Sagnac frequency (10-20 ppm of Earth rotation) for 1-second samples.

Coupling mechanisms and relative phase

Possible mechanisms coupling seismic waves to a ring laser were considered in earlier work [*McLeod et al.*, 1998]. A ring laser detects the Sagnac beat frequency between counter-propagating beams:

$$\delta f + \delta f_v = \frac{4A\,\hat{\mathbf{n}}\cdot(\mathbf{\Omega_E} + \mathbf{\Omega_D})}{\lambda P} \qquad (1)$$

where the seism-independent base term δf arises from Earth rotation $\mathbf{\Omega_E}$ alone and has the value 79.40 Hz in C-II and 288.2 Hz in G0, δf_v covers all correction terms arising from seismic effects, $\mathbf{\Omega_D}$ is the seismically induced additional local rotation (vorticity), P, A, and $\hat{\mathbf{n}}$ are the perimeter, area magnitude and the (unit vector) orientation (of the area vector $A\hat{\mathbf{n}}$) of the ring. The HeNe optical wavelength λ = 633 nm. Each of P, A and $\hat{\mathbf{n}}$ is affected by seismic deformations from the base value distinguished by a subscript 0. Hence seismic coupling terms within δf_v arise separately and in combination [*McLeod et al.*, 1998]. The effects of seismic strain (on A/P) and of tilt (on the scalar product) were both less than seismically induced changes in rota-

Paper number 1999GL000000.
0094-8276/00/1999GL000000$05.00

Table 1. Parameters for the New Ireland and Vanuatu events (figure 1) discussed. Δ is the angular distance between epicentre and ring laser, ϕ the back azimuth, and M_W is the moment magnitude. All angle units are degrees.

Location	Date and time (UT)	M_W	Δ	ϕ
New Ireland	1999 Jan 19 03:35:33.8	7.0	42.6	330.54
Vanuatu	1999 Feb 6 21:47:59.1	7.3	31.0	348.70

tion rate $\delta f_{vor} = 4A_0\,\hat{\mathbf{n}}_\mathbf{0}\cdot\boldsymbol{\Omega}_\mathbf{D}/\lambda\mathbf{P_0}$ by factors of the order of $\Omega_E/\omega \sim 2\times10^{-4}$, where ω is the teleseismic frequency, so that δf_{vor} was expected to dominate by a factor ~ 5000.

We mention two corrections to our earlier work [*McLeod et al.*, 1998]. The work quoted therein, [*Stedman et al.*, 1995], indicates that a factor $\frac{1}{2}$ is needed for a simple shear wave, making Equation (8) of [*McLeod et al.*, 1998] $\Omega_{\max} = 2\pi^2 a/c_s T^2$ for an SH wave. Second, strain has a much larger effect on the Sagnac frequency than estimated from the factor A/P because of backscatter-induced frequency pulling [*Schreiber et al.*, 1999]. However, this does not affect either ring laser being a gyroscope for seismic purposes. In C-II, seismic strain is decoupled from the monolithic Zerodur resonator via teflon pads, and in G0 frequency pulling is dispersion-related rather than backscatter-dominated, correlating with mode swapping rather than with ambient pressure.

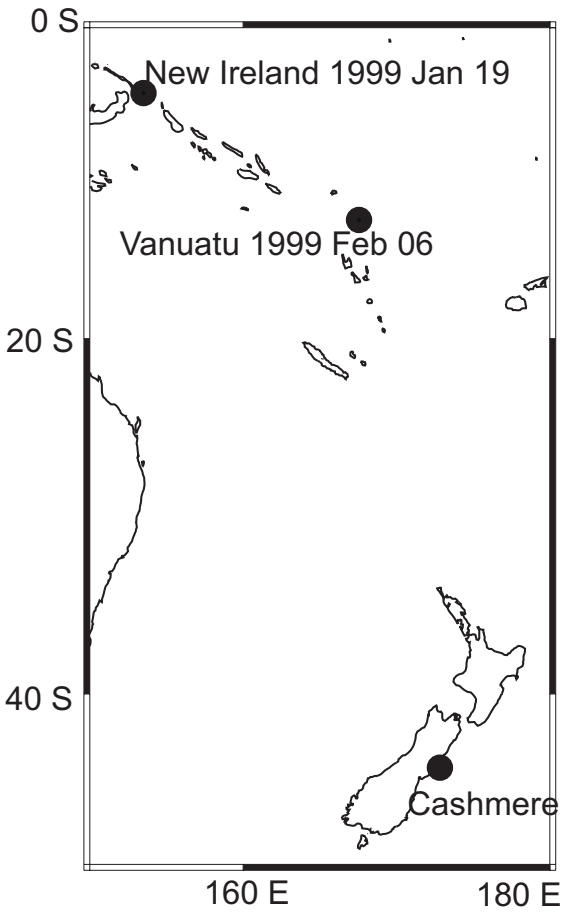

Figure 1. Locations of the New Ireland (4.57 S, 153.18 E) and Vanuatu (13.00 S, 166.70 E) events discussed. Parameters are given in Table 1.

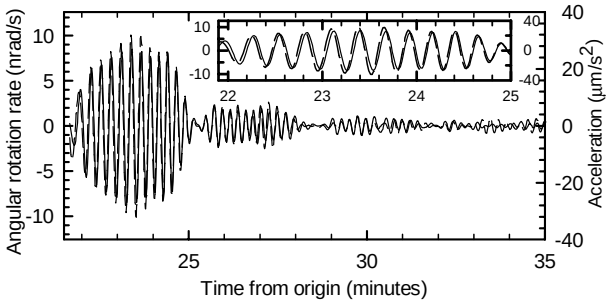

Figure 2. Anticlockwise angular rotation rate Ω about a vertical axis (solid line) and transverse acceleration (dashed), as measured by C-II and EARSS/40T respectively, for New Ireland,1999 Jan 19 03:35:33.8 UTC. In the inset plot, which has the same axis labels, the traces are overlaid to show their phase relation.

We now consider the expected phase relationships between contributions to δf_v. Taking a wave with linear polarisation $\mathbf{e}$ for simplicity, we let the local surface motion be $\mathbf{u}(\mathbf{x},\mathbf{t}) = \mathbf{u_0 e}\sin\phi$ where $\phi = \omega t - \mathbf{k}\cdot\mathbf{x}$ and u_0 is the amplitude. A linear velocity sensor in a seismometer will deliver a signal varying as $\mathbf{v} = \mathbf{v_0 e}\cos\phi$ with $v_0 = \omega u_0$. The acceleration (derived in practice from the velocity record by multiplying by frequency in the Fourier domain) will be $\mathbf{a} = -\mathbf{a_0 e}\sin\phi$ with $a_0 = \omega^2 u_0$. The components of the strain tensor $\varepsilon_{ij}(t) = \frac{1}{2}\left(\partial u_i/\partial x_j + \partial u_j/\partial x_i\right)$ therefore have a factor $\cos\phi$, as does the rotation amplitude (including tilt) $\theta = \frac{1}{2}\nabla\times\mathbf{u}$. Hence the alternative coupling mechanisms which were predicted by McLeod *et al.* to be small have (modulo a sign) the same phase as the velocity, whereas rotation rate $\boldsymbol{\Omega} = \dot{\theta} = \frac{1}{2}\omega\mathbf{u_0 e}\times\mathbf{k}\sin\phi$ and is in phase with displacement and acceleration. The observations reported here discriminate amongst these possibilities, and also give more information on the relative amplitudes. In the above theory the rotation rate amplitude is $\Omega_0 = \frac{1}{2}\omega k u_0$, and acceleration has the relative amplitude $a_0/\Omega_0 = 2c_s = 2\omega/k$, or double the phase speed of the wave.

Signal processing techniques

A Guralp CMG-40T linear seismometer was sampled at 50 Hz and seismic triggers were provided by an EARSS seismograph [*Gledhill et al.*, 1991]; we distingush this system by EARSS/40T. The signals from the ring laser beam combiners were sampled at 800 Hz, with signal/noise typically 60 dB or better. When EARSS triggers were available (normally only at the S arrivals) both data streams were jointly recorded at 800 Hz. All EARSS data has been post-filtered to remove the long-period falloff in response of the EARSS/40T system. For phase comparisons, a relatively monochromatic teleseismic wave was isolated by band-pass filtering (30-80 mHz). Sagnac frequencies are estimated from 1-Hz AR(2) analysis and their teleseismic content selected by the above band-pass filtering. The Sagnac frequency data δf are converted to actual angular rotation rate Ω for the final plots using equation (1); for a square ring laser, $\Omega = 4\lambda\,\delta f/P$. Acceleration data from the EARSS system is rotated into the transverse direction, the posi-

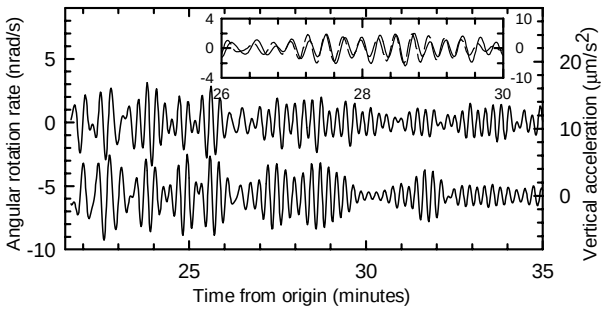

Figure 3. Anticlockwise angular rotation rate about a horizontal axis and vertical acceleration, as measured by G0 and EARSS/40T respectively, for New Ireland,1999 Jan 19 03:35:33.8 UTC. In the main plot, the upper curve is the rotation rate. In the inset plot, which has the same axis labels, the traces are overlaid to show their phase relation; the acceleration curve is dashed.

tive direction being 90° clockwise to the direction of propagation of the incident wave. This corresponds to an anticlockwise rotation of a horizontal laser, i.e. a reduction of Earth rotation; this phase change has been applied to the laser data, making the predicted relative phase zero. Results from G0, which is vertical, are compared with the vertically upward component of acceleration; however the oblique incidence, vertical dependence of amplitude and elliptical polarisation of the Rayleigh waves mean that other components of ground motion could also be relevant.

The noise floors of such instruments can be quantified using for example the rotation sensitivity S or the power spectral density [*McLeod et al.*, 1998]. Here we quote the Allan deviation, the standard deviation of Sagnac frequency differences as a function of sampling time τ, relative to the Sagnac frequency from Earth rotation during the period of the runs discussed below. These deviations are typically 10-20 ppm for G0 over $1 < \tau < 100$ s, and ~ 6 ppm for C-II for $20 < \tau < 100$ s.

New Ireland earthquake, 1999 January 19

We discuss here two events in which teleseismic waves were observed, as given in Table 1. The locations of these events are depicted in figure 1.

The New Ireland earthquake has origin time 1999 January 19, 03h 35m 33.8s. A data logging run commencing at 03h 57m 12.4s immediately recorded surface waves in both C-II and G0 (figures 2, 3 respectively). This data run missed the body waves and the Love wave first arrival (at approximately 18.5 minutes) but captured earlier parts of the Love wave (figure 2), and later parts of the Rayleigh wave (figure 3).

The phase difference between the linear and rotational forms of teleseismic waves was estimated by fitting a sinusoid for each 10-second interval and taking an amplitude-weighted average. The net phase difference for the horizontal case (figure 2) was -26° ± 9°, the quoted error being the scatter in the estimates. For the vertical case (figure 3) the comparison yields a net phase difference of -39° ±36°. These empirical results certainly favour a value 0 mod π for the phase difference over $\pi/2$ mod π; the systematic difference from zero suggests a residual unaccounted instrumental effect. This data supports the view that both C-II and G0 respond to rotation rate rather than to either tilt or strain amplitude, for which we would expect a $\pi/2$ phase difference ($\cos\phi$ rather than $\sin\phi$).

The maximum amplitudes of EARSS/40T and C-II response from figure 2 have the ratio $a_0/\Omega_0 \sim 3.3$ km/s. From the above theory, applicable for a Love wave (since its surface coordinate dependence has the trigonometric form assumed regardless of its depth dependence), a_0/Ω_0 is expected to be twice the phase speed (3.5 km/s for Love waves). Since the observed values are a factor of 2 less than this, the induced rotations are larger than expected for the measured acceleration.

For G0, the observed rotation rate relative to the acceleration is very much larger again; the maximum amplitudes of EARSS/40T and G0 response from figure 3 have a ratio $a_0/\Omega_0 \sim 1.6$ km/s. For a Rayleigh wave, the calculation of [*Stedman et al.*, 1995] gives an enhancement of the rotation rate Ω_0 over the simple model by the factor $\sqrt{1+\sqrt{3}} = 1.65$. This enhancement factor is comparable with the observed further lowering of the ratio a_0/Ω_0 in G0 data over C-II data; however the oblique mounting of G0 requires a more detailed analysis of the relationship between the acceleration components and net rotation rate than we attempt here.

Vanuatu earthquake, 1999 February 06

Table 1 and Figure 1 give the parameters for this event. The data acquisition system triggered on the P wave. Figure 4 gives C-II and EARSS/40T band-filtered records; G0 was offline on this occasion. There is a 6.72-minute data gap in the ring laser and joint record. The data are bandpassed 0.03-0.08 Hz to clarify the phase relationship in the main phase. The noise floor ($\sim$ 0.3 nrad/s/$\sqrt{}$Hz) is ring-laser (shot noise) related, not ground noise, and in the angular velocity domain a factor 30 less than the noise floor ~ 3 nrad/s^2/$\sqrt{}$Hz reported in this frequency regime for a high-sensitivity rotational accelerometer [*Luiten et al.*, 1997] .

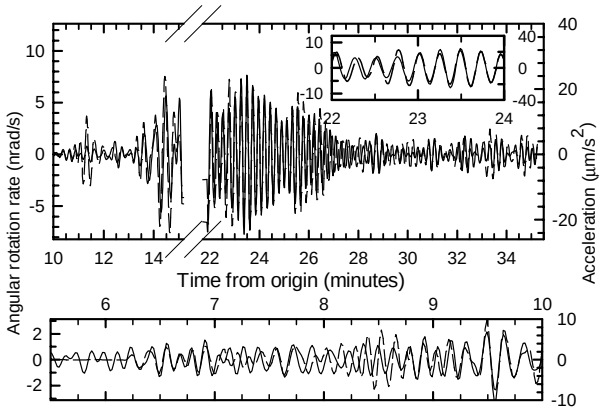

Figure 4. Anticlockwise angular rotation rate about a vertical axis (solid line) and transverse acceleration (dashed), as measured by C-II and EARSS/40T respectively, for Vanuatu,1999 Feb 6 21:47:59 UTC. The various plots differ in their time axes and in the bandpass filterings chosen, as discussed in the text.

The phase difference averaged over the major waves is -3° ± 31°; as the inset figure illustrates, this result supports a null value and the rotational coupling model. The amplitude ratio of EARSS/40T and C-II response from figure 4 is $a_0/\Omega_0 = 2.8$ km/s. This ratio is consistent with the New Ireland results for C-II, being roughly half the theoretical expectation. This is a challenge for further study; the factor arises on comparison of two very different instruments, so that calibrations and seismic speeds, though checked, could all conceivably contribute to this systematic shift.

Body waves were recorded in this event. The arrival of the S wave at 11.5 minutes is conspicuous in both records (Figure 4); its comparative weakness in the ring laser record may reflect its steep angle of incidence (26 deg. to the vertical) and consequent lack of effectiveness for horizontal rotation. The EARSS/40T transverse seismogram also shows significant energy from the time of the first P wave arrival. Other than for the direct P wave, this energy cannot be removed by rotating the seismograms into different back azimuths, although the true back azimuth may vary with time. The amplitude of the transverse waveform increases with time (and does not correlate with the larger amplitude signals on the radial and vertical components). This implies that it was converted to S some distance from the receiver, perhaps at the dipping North Island subduction zone interface. Also shown is the C-II rotation rate plotted on the same relative scale as in the upper figure; the data are bandpassed 0.05-0.15 Hz to capture the earlier components. The signal-to-noise ratio is lower for C-II than for the EARSS/40T system, but some rotational response can be seen early in the P wave coda. The amplitude of the rotation rate is rather lower than the transverse acceleration record would suggest for portions of the period 8-10 minutes after the origin time. This could either be because the transverse coda includes significant P/SV energy (off azimuth) as well as SH, or because SH energy, even if dominant, is steeply incident.

This analysis confirms the gyroscopic interpretation of ring laser detection of teleseismic waves, and gives considerable impetus to further detection of body waves, coda, and surface waves in teleseismic events. The fact that the measured rotation rates are rather larger than expected enhances the interest of these results.

Acknowledgments. We thank Tim O'Neill and Ken Gledhill for help with data collection and Mark Chadwick for help with instrument responses. The C-II ring laser results were possible because of a collaboration of Forschungseinrichtung SatellitenGeodäsie, Technische Universität München, Bundesamt für Kartographie und Geodäsie, Frankfurt, and University of Canterbury, Christchurch, New Zealand; University of Canterbury research grants U6292, U6332, also contracts UOC 513 and 802 of the Marsden Fund of the Royal Society of New Zealand. D. P. McLeod acknowledges receipt of a University of Canterbury Postgraduate Scholarship.

References

Gledhill K. R., M. J. Randall and M. P. Chadwick. The EARSS digital seismograph: system description and field trials, Bull. Seis. Soc. Am. **81**, 1380-1390, 1991.

Kennett, B.L.N., IASPEI 1991 Seismological Tables (Research School of Earth Sciences, Aust. Natl. University, 1991).

Luiten A. N., Beccaria, M. Bernadini, M. and 30 others, Ground tilt seismic spectrum measured with a new high sensitivity rotational accelerometer , Rev. Sci. Instrum. **68**, 1889-1893, 1997.

McLeod, D.P., Stedman, G. E., Webb, T. H., and Schreiber, U. K., Comparison of standard and ring laser rotational seismograms, *Bull. Seism. Soc. Am.* 88, 1495-1503, 1998.

Rowe, C. H., Schreiber, U. K., Cooper, S. J., King, B. T., Poulton, M., and Stedman, G. E. Design and operation of a very large ring laser gyroscope *Appl. Opt.* 38, 2516-2523, 1999.

Schreiber, U. K., Rowe, C. H., Wright, D. N., Cooper, S. J., and Stedman, G. E. Precision stabilization of the optical frequency in a large ring laser gyroscope, *Appl. Opt.* 37, 8371-8381, 1998.

Schreiber, U. K., Schneider, M., Rowe, C. H., Stedman G. E. and Schlüter, W., Stabilising the operation of a large ring laser, *Proceedings of the Symposium Gyro Technology* ed. H Sorg (Universität Stuttgart, Institut A für Mechanik, Stuttgart, September 1999).

Stedman, G.E., Li, Z., and Bilger, H. R. Sideband analysis and seismic detection in large ring lasers, *Appl. Opt.* 34, 7390-7396, 1995.

Stedman, G. E., Ring laser tests of fundamental physics and geophysics, *Reports Progr. Phys.* 60, 615-688, 1997.

Takeo, M., Ito, H. M. What can be learned from rotational motions excited by earthquakes? *Geophys. J. Int.* 129, 319-329, 1997.

G. E. Stedman, D. P. McLeod, Department of Physics and Astronomy, University of Canterbury, Private Bag 4800, Christchurch, New Zealand (e-mail: g.stedman@phys.canterbury .ac.nz)

A. Pancha, T. H. Webb, Institute of Geological and Nuclear Sciences, P.O. Box 30-368, Lower Hutt, New Zealand. (e-mail: terry.Webb@gns.cri.nz)

K. U. Schreiber, Fundamentalstation Wettzell, Sackenriederstrasse 25, D-93444 Kötzting, Bavaria, Germany. (e-mail: schreiber@wettzell.ifag.de.)

(Received May 1, 2000; revised June 12, 2000;
accepted July 28, 2000.)